Reprinted from COMBUSTION SCIENCE AND TECHNOLOGY, Vol. 97, No. 1-3, 37-62, 1994

Combust. Sci. and Tech., 1994, Vol. 97, pp. 37-62
Photocopying permitted by license only

Heat Feedback to the Fuel Surface in Pool Fires

A. HAMINS, S. J. FISCHER and T. KASHIWAGI *Building and Fire Research Laboratory, National Institute of Standards and Technology, Gaithersburg, MD 20899*

M. E. KLASSEN and J. P. GORE, *School of Mechanical Engineering, Purdue University, West Lafayette, IN 47907*

(Received April 10, 1991; in final form February 26, 1993)

Abstract—A series of measurements designed to investigate the heat feedback in pool fires burning liquid fuels are reported. Such measurements are essential for the development and validation of detailed models which predict the burning rate of liquid hydrocarbons and solid polymers. The radial variation of the local radiative and local net heat flux incident on the surface of 0.30 m diameter pool fires were measured. A water-cooled, nitrogen purged, narrow view-angle gauge was developed to measure the radiative flux incident on the fuel surface. Measurements of the mass burning rate in a burner composed of annular rings was used to estimate the local heat feedback. A number of different fuels were studied, yielding flames with a wide range of heat release rates and luminosities. Consideration of the heat balance for a control volume enclosing the liquid pool indicated that radiation was an important component of the heat feedback for non-luminous fires and a dominant component in luminous fires.

1. INTRODUCTION

The heat flux to the surface of a pool fire and the mass flux vaporizing from the pool are part of a positive feedback loop. The rate of mass burning depends on the heat feedback from the flame to the fuel surface, and the mass burning rate controls the total heat release rate and the amount of heat feedback. The ratio of the heat per unit time ($\dot{Q}_{fuel}$) needed to vaporize the fuel, to the ideal combustion heat release rate ($\dot{Q}_{chem}$) is the heat feedback fraction (χ_s):

$$\chi_s = \dot{Q}_{fuel}/\dot{Q}_{chem} \tag{1}$$

For a steadily burning fire, $\dot{Q}_{fuel}$ can be approximated as:

$$\dot{Q}_{fuel} = \dot{m} \cdot (H_v + C_p \cdot (T_s - T_o)) \tag{2}$$

where $\dot{m}$ (g/s)is the fuel burning rate, H_v (J/g) is the heat of vaporization, C_p (J/g-K) is an average specific heat of the liquid fuel taken at $[T_s + T_o]/2$, T_s (K) is the pool surface temperature and T_o (K) is the ambient temperature. $\dot{Q}_{chem}$ (W) is defined as:

$$\dot{Q}_{chem} = \dot{m} \cdot H_C \tag{3}$$

where H_c (J/g) is the ideal heat of combustion. As designated, χ_s is the reciprocal of the diffusive transfer number cited in the literature (Spalding, 1955; Burgess and Hertzberg, 1974). The value of χ_s is independent of the mass burning rate and depends mainly on intrinsic molecular properties. Table I shows that χ_s varies more than a factor of five among common liquid fuels.

Heat feedback from the flame to the fuel surface occurs through radiative, convective and conductive heat transfer. The relative contributions of these heat feedback processes may depend on a large number of factors, including the pool diameter, the flame shape,

TABLE I

Pool fire properties including the average mass burning rate ($\dot{m}$), heat feedback fraction (χ_S), radiative heat release fraction (χ_R), idealized heat release rate ($\dot{Q}_{chem}$), radiative heat loss rate ($\dot{Q}_{emit}$), the measured time averaged flame height (H_{exp}), and flame height estimates (H_z and H_H) from Zukoski (1984) and Heskestad (1983) respectively.

Fuel	$\dot{m}$	χ_S	χ_R	$\dot{Q}_{chem}$	$\dot{Q}_{emit}$	H_{exp}	H_z	H_H
	(g/s)			(kW)	(kW)	(m)	(m)	(m)
heptane	2.6	0.010	0.31	116	36	1.31	1.33	1.28
methyl alcohol	0.92	0.054	0.20	21	4.2	0.51	0.52	0.44
MMA	2.7	0.017	0.32	73	23	0.96	1.11	0.94
toluene	3.1	0.012	0.26	130	39	1.05	1.39	1.31

the flame luminosity, and the spatial distribution of temperature and soot inside of the fire.

1.1 Heat Balance

A schematic diagram of the heat balance in a liquid fuel pool fire is shown in Fig. 1 for a quasi-steady state system. Such a system is achieved by adding fresh fuel into the pool bottom such that the fuel level remains constant. A short time after after ignition ($\approx$ 5 min for 0.30 m pool fires), the fuel burning rate ($\dot{m}$) in such a system is nearly constant, but the temperature throughout the pool continues to gradually increase.

The width of the arrows in Fig. 1 symbolize the approximate importance of each of the terms in the heat balance occurring in a 0.30 m heptane pool fire. The net heat feedback per unit time, $\dot{Q}_{net}$ (W), to the pool surface, dominated by the sum of convection ($\dot{Q}_{conv}$) and radiation ($\dot{Q}_{rad}$) is balanced primarily by $\dot{Q}_{fuel}$ (see Eq. 2). A detailed heat balance must consider other thermal sources and sinks. These include heat gain due to conduction through the metal burner walls, heat losses due to radiation from the fuel surface to the surroundings ($\dot{Q}_{rerad}$), losses from the bottom and sides of the burner ($\dot{Q}_{loss}$), and reflection of a portion of the radiation incident on the pool surface ($\dot{Q}_{reflect}$) which is dependent on the angle of incidence and the refractive index of the fuel. A heat balance for a control volume about the liquid pool can be represented as:

$$\dot{Q}_{net} = \dot{Q}_{cond} + \dot{Q}_{conv} + \dot{Q}_{rad} - \dot{Q}_{reflect} \tag{4}$$

$$= \dot{Q}_{fuel} + \dot{Q}_{rerad} + \dot{Q}_{loss} + \dot{Q}_{corr} \tag{5}$$

The loss terms ($\dot{Q}_{rerad}$ and $\dot{Q}_{loss}$) act to diminish the fraction of energy available for fuel vaporization, but are typically small when compared to $\dot{Q}_{fuel}$. A term associated with the gradual growth of the thermal layer inside of the liquid pool ($\dot{Q}_{corr}$) must also be considered. Another possible contribution to the overall heat balance is from water condensation ($\dot{Q}_{water}$) on the fuel surface. Condensation of gas-phase water molecules, diffusing from the flame towards the relatively cool fuel surface, could impact the fuel burning rate measurement and would increase the enthalpy of the pool. This term may be non-trivial for fuels with pool surface temperatures (T_s) significantly less than the water boiling point ($T_s << 373$ K).

1.2 Previous Studies

Previous measurements of the local radiative or net heat flux at the surface of pool fires are listed in Table II. Measurements have been conducted on pools varying in

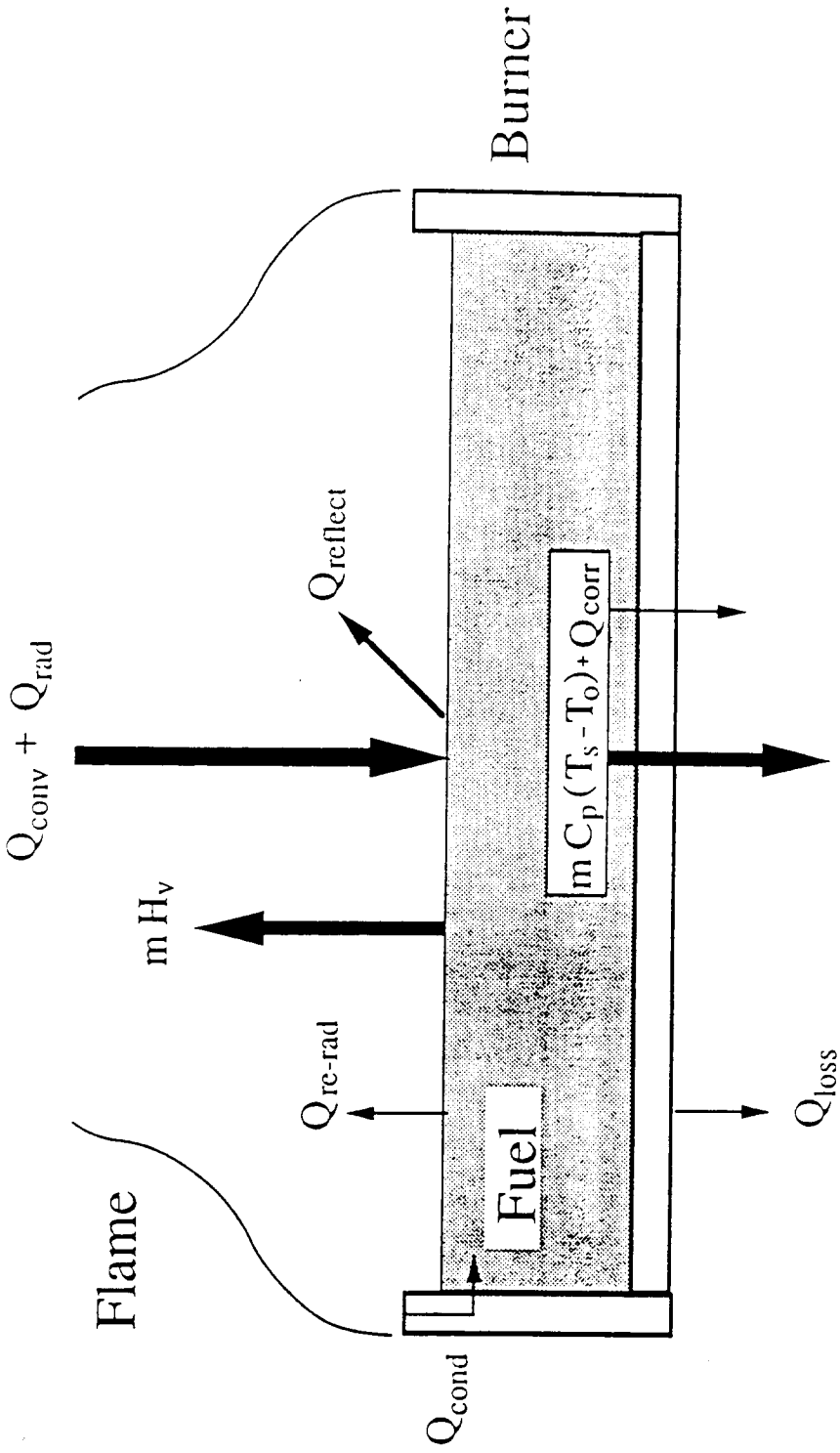

FIGURE 1 Schematic drawing of the energy balance for a pool fire burning a liquid fuel.

TABLE II
Previous Studies on Heat Feedback in Pool Fires

AUTHOR	FUEL	DIAMETER (m)	$\dot{Q}''_{rad}$	$\dot{Q}''_{net}$	STEADY STATE	COMMENTS
Blinov & Khudyakov (1961)	benzene gasoline kerosene oil	0.03-.8		X	YES	ring pool burner
Corlett & Fu (1966)	methanol acetone	0.006-0.3	X		YES	insulated fuel well
Akita & Yumoto (1965)	methanol	0.1-0.3	X		YES	ring pool burner
Thomas et al. (1965)	ethanol	0.9	X	X	NO	dual gardon gauge
Yumoto (1971)	gasoline hexane	0.6-3	X	X	YES	pool center only
Modak & Croce (1977)	PMMA	0.2		X	NO	recession rate
Alger et al. (1979)	methanol JP-5	3	X		NO	Gardon & transpiration gauges
Shinotake et al. (1985)	heptane	0.3-1	X	X	NO	dual Gardon gauges

diameter (D) from $\approx$ 0.01 to 3 m for a number of different liquid fuels and a solid, polymethylmethacrylate (PMMA). Studies of local mass burning rates were conducted using ring pool burners (Akita and Yumoto, 1965; Blinov and Khudyakov, 1961) and insulated fuel wells (Corlett and Fu, 1976). Local radiative heat fluxes were measured using dual Gardon gauges (Yumoto, 1971; Shinotake et al., 1985) or aspirated radiometers (Alger et al., 1979).

Akita and Yumoto (1965) observed the burning rate of methyl alcohol in two pans (D=0.18 m and 0.29 m) each consisting of three concentric equal area rings. In both cases, an additional outer ring was filled with water. The fuel burning rate was measured in each ring while the liquid level was maintained at a constant height (a quasi steady state system). Akita and Yumoto's measurements show that the burning rate was incrementally higher towards the edge of pool fires burning methyl alcohol in the two ring burners. From these measurements, they concluded that radiative heat feedback was negligible compared to convective and conductive heating of the pool. Assuming zero radiative feedback to the liquid pool, empirical local heat transfer coefficients were introduced and the burning rate data were favorably compared to Hottel's (1958) theory of mass burning rates for luminous flames.

In their extensive investigation of pool fires, Blinov and Khudyakov (1961) measured the burning rate of a number of hydrocarbon fuels in burners consisting of concentric rings. Three different burners were used, including a 0.80 m and a 0.30 m four-ring burner.

Fuels tested included benzene, gasoline, kerosene and diesel oil. For all fuels, the burning rates were highest in the center ring, decreased away from the center and increased in the outer ring. These results were qualitatively different from the measurements reported by Akita and Yumoto (1965). All of the fuels tested were highly luminous, unlike the soot-free methyl alcohol fires studied by Akita and Yumoto. It is conceivable that the spatial variation of mass burning rates in soot-laden pool flames may be entirely different than methyl alcohol fires.

Burgess and Hertzberg (1974) used Hottel's (1958) bulk properties formulation for pool burning and Blinov and Khudyakov's (1957) burning rate data, and determined that radiative transfer becomes dominant over convection at pool diameters of 0.1 to 0.5 m depending on fuel type. Below these sizes convection was considered very important.

A global approach to radiative flame modeling has been used by a number of investigators including Modak (1977), who described the radiative heat flux from the flame to a surface element on the burning pool in terms of an empirical time-averaged flame shape, an effective radiation temperature, and a mean gray body absorption-emission coefficient. For conditions in a 0.18 m pool of PMMA, radiative heat feedback to the pool surface was calculated and found to monotonically decrease from the pool center towards the pool edge. From a net heat flux measurement at the pool center and a radiant flux calculation, Modak (1977) found that the convective heat transfer was about 5% of the radiative transfer at the pool center for the PMMA fire. An expression describing radiative flux to the PMMA pool surface as a function of radial location (for a cylindrical flame shape) was favorably compared to the time-averaged local burning rate data for a number of PMMA pool fires (Modak and Croce, 1977).

Other studies have measured radiative heat transfer to the surface of liquid pool fires. Yumoto (1971) measured heat feedback to intermediate-sized ($0.6\ m < D < 3.0\ m$) gasoline and hexane pool fires using dual Gardon gauges with different emissivities, but measurements were made at the pool center only. Alger et al. (1979) measured the radiative feedback to large scale (3 m) methyl alcohol pool fires using Gardon and transpiration radiometers at several pool locations. They found that the radiation decreased from the pool center towards the pool edge by almost a factor of two. Shinotake et al. (1985) determined convective and radiative heat feedback near the center of intermediate sized pools burning heptane by use of dual Gardon gauges with different surface emissivities. Their results showed that nearly 65% of the heat feedback near the pool center was due to radiation in their 0.3 m heptane fire. In those experiments, however, a thin fuel layer was floated over water, and the fuel was not maintained at a constant level with relation to the burner rim. Corlett and Fu (1966) estimated the local radiative heat transfer at several locations on the surface of methyl alcohol and acetone pool fires ($0.05\ m < D < 0.225\ m$) using a small insulated well filled with fuel, but only a few measurements near the pool center were conducted.

Experimental characterization of the local heat transfer to the pool surface is essential for the development and validation of detailed models which predict the burning rates of liquid hydrocarbons and solid polymers. Yet, only a limited number of experiments have measured local heat transfer to the fuel surface. The objective of the present work was to characterize systematically the heat feedback to the surface of 0.30 m pool fires. Specifically, measurements of the radial variation of both the mass burning rate and the radiative heat flux were conducted. A number of fuels were tested, yielding flames with a wide range of heat release rates ($21\ kW < Q_{chem} < 130\ kW$) and luminosities as listed in Table I.

2. EXPERIMENTAL APPARATUS AND METHOD

Table III lists the operating conditions of the experiments conducted in this study. Two types of pool burners were used; a simple 0.30 m (outer diameter) burner and two

TABLE III
List of experiments described in the text.

Measurement	Burner	Fuels	Lip height (cm)
$\dot{m}$ (g/s)	four-rings	heptane	0.5
		toluene	0.5
		methanol	0.1, 0.5
		MMA	0.5
$\dot{m}$ (g/s)	five-rings	heptane	0.5
$\dot{m}$ (g/s)	water in fifth ring	methanol	0.5
$\dot{Q}''_{rad}$ (kW/m^2)	simple (no rings)	heptane	0.5
		toluene	0.5
		methanol	0.5
$\dot{Q}''_{net}$ (kW/m^2)	simple (no rings)	heptane	0.5
		toluene	0.5
		MMA	0.5

annular ring burners (0.30 m and 0.38 m outer diameter, composed of four and five annular rings respectively). The ring burners, identical to the simple burner in all aspects except for the annular rings, were used to make mass burning rate measurements for four fuels including heptane (C_7H_{16}), toluene (C_7H_8), methyl alcohol (CH_3OH) and methyl methacrylate, MMA ($C_5H_8O_2$).

The simple burner was used to measure the radiative heat flux at the surface of pools burning toluene, heptane, and methyl alcohol. These fuels were chosen because of the large differences in the radiation characteristics of the resulting flames. A schematic of the experimental facility and the ring burner is shown in Fig. 2. All burners were made of stainless steel, water cooled (289K) at the bottom, 0.15 m in depth, located under a water cooled hood, and burned in an enclosure made of double wire mesh walls (1.8 m long, 1.6 m wide and 2.1 m high) to minimize convective currents in the room. The four ring burner consisted of concentric rings of 0.077, 0.152, 0.229, and 0.303 m outer diameter, giving annular surface area ratios of 1:4:9:16, from inner to outer rings. The ring walls were 0.0016 m thick. A second ring burner, identical to the first, but with a fifth (fuel or water filled) annular ring (0.381 m outer diameter) was used in a number of experiments. The fuel in all experiments was gravity fed to the burner. The output of chromel-alumel thermocouples (located 5 mm above the fuel surface) controlled the operation of solenoid valves in the fuel lines, and allowed adjustment of the level of the liquid fuel, generally maintained 0.5 cm below the rim of the burner. The uncertainty in lip height was estimated to be 0.1 cm except for toluene in the ring burner, when direct visual observation of the liquid level in the center ring was obscured by the highly luminous and sooty fire. The fuel for each ring was stored in a separate reservoir, each resting on a load cell (0.1 g repeatability); and the mass loss rates were monitored by a digital voltmeter and stored on computer. The uncertainty in the load cell data was estimated to be $\pm 5\%$ based on repeated measurements and calibrations using known weights.

A typical experiment consisted of a 10 minute warm-up period and a 25 to 45 minute observation time. The measured mass burning rates in both burners were nearly constant after the warm-up period. Mass burning rate measurements were repeated at least five times for each fuel.

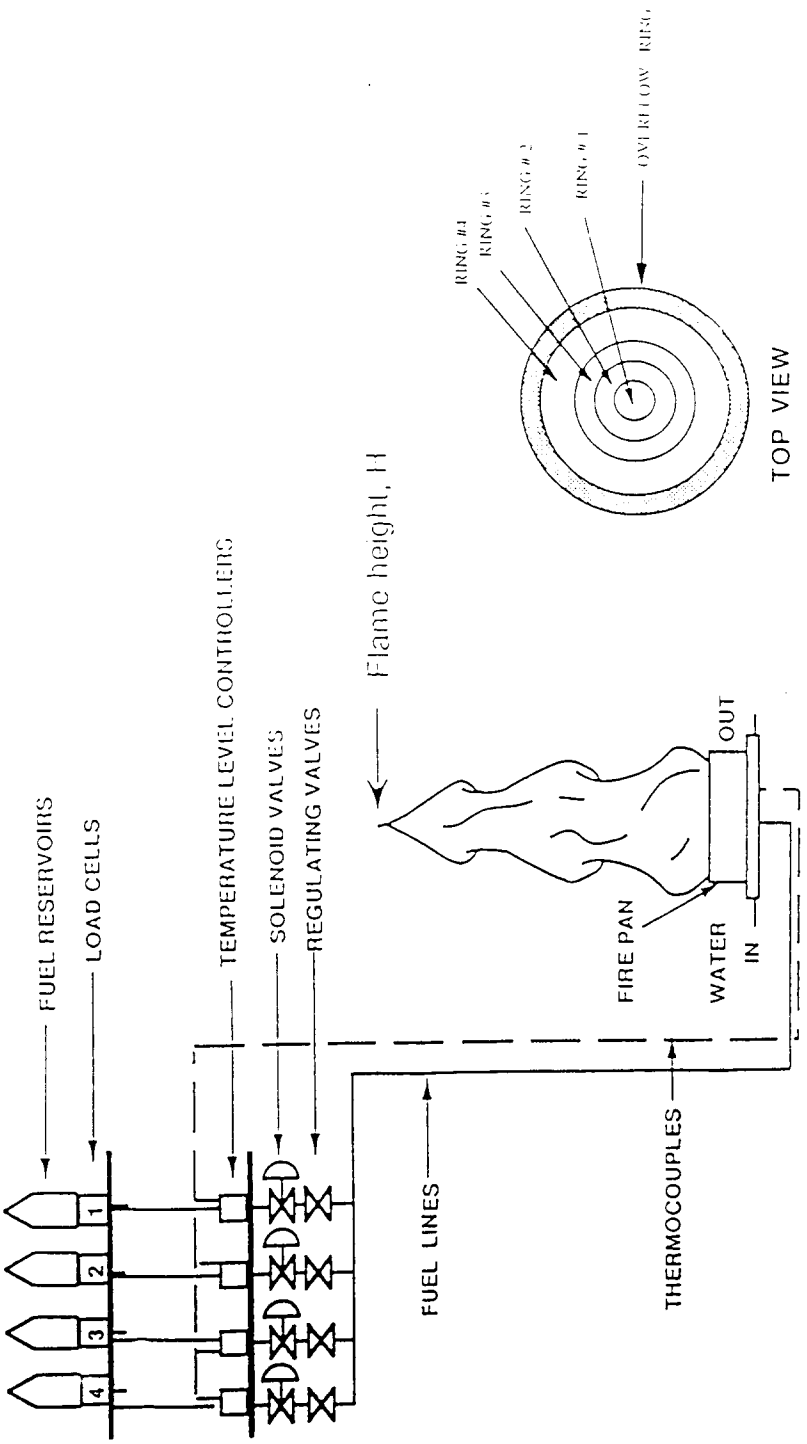

FIGURE 2 Schematic drawing of the fuel feed system for an annular ring pool burner. Also shown is a top view of the burner.

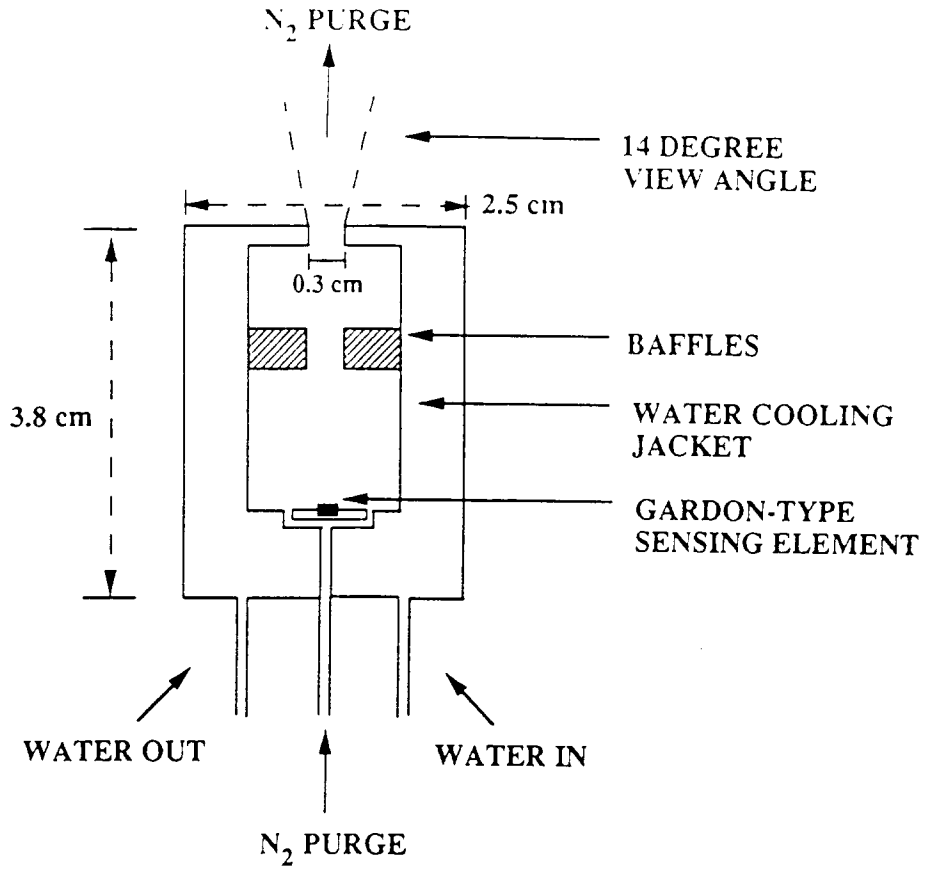

FIGURE 3 Schematic drawing of the narrow view-angle, water cooled, windowless, nitrogen purged radiative heat flux gauge.

2.1 Radiative Heat Flux Gauge

A narrow view-angle radiometer was used to measure the radiative flux at the pool surface. Figure 3 shows the radiative heat flux gauge which was 0.025 m diameter, 0.038 m long, water cooled and windowless. A nitrogen purge (33 cc/s) prevented fuel from diffusing back and condensing on the sensing element. Momentary reduction of the nitrogen to a near zero flow rate showed that the purge had a negligible effect on the measured radiation. A set of baffles defined the view-angle which was measured to be 0.004 str or ±7° (full width at half maximum).

Measurements along the pool surface were made every 0.02 m and tilted at 20° intervals from $\Theta = 30°$ to $\Theta = 150°$ for $\phi = 0°$ and from $\Theta = 30°$ to $\Theta = 90°$ for $\phi = 90°$, where the angles are defined as shown in Fig. 4. The heat flux gauge was placed into the pool such that the top center of the gauge was approximately 0.007 m above the fuel surface (0.002 m above the plane defined by the burner rim). For locations near the pool edge and for small angles ($\Theta = 30°$), the gauge was positioned outside of the pool. Measurements were made at a 30 Hz sampling rate for 90 seconds per measurement. The radiometer was calibrated using a black body light source (1273 ± 1 K) and a standard heat flux meter. The background signal of the radiative heat flux gauge was

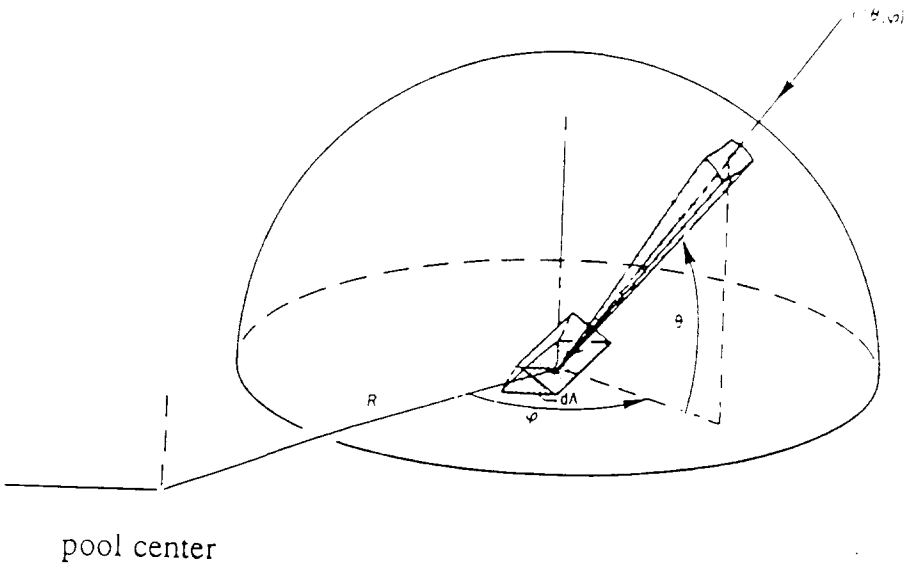

FIGURE 4 Schematic drawing defining the direction viewed by the narrow view-angle radiative heat flux gauge.

measured in situ, with the fire burning, by placing a water cooled cap on the gauge with the nitrogen purge flowing. Small differences in the background signal were measured as the direction and location of the gauge were changed.

It was determined that higher temperature cooling water ($\approx$ 363 K) was needed to prevent attenuation of signal from the radiative heat flux gauge in the toluene fire, presumably due to fuel and/or water condensation inside of the gauge. The higher temperature cooling water, however, influenced the fuel mass burning rate causing it to increase approximately 25%. Cooling the gauge with room temperature water did not significantly affect the fuel burning rate in the methyl alcohol or the heptane fires as compared to the total mass burning rate in the ring pool burner.

2.2 *Reflected Radiation*

A series of experiments measured the amount of reflected infrared radiation from the liquid surface as a function of incident angle. A schematic diagram of the experimental arrangement is shown in Fig. 5. A blackbody (1273 K) radiation source was reflected from a rotating mirror onto the surface of the liquid pool at room temperature (296 K). A number of liquid fuels and water were tested. The reflected infrared radiation was measured as a function of reflected angle by a lead sulfide (PbS) detector. Although these measurements were conducted at room temperature, the index of refraction of the liquids is not expected to change as the temperature at the surface of the burning pool approaches the fuel boiling point. Discoloration of the fuel due to soot deposition in the heptane and toluene fires was assumed not to alter the liquid index of refraction.

2.3 *Local Total Heat Flux*

A wide view-angle, water cooled, total heat flux (Gardon) gauge with a 1.3 cm diameter face (and a 0.4 cm diameter sensing element) was used to measure heat flux to the surface of the liquid pools burning MMA, heptane and toluene. In these experiments,

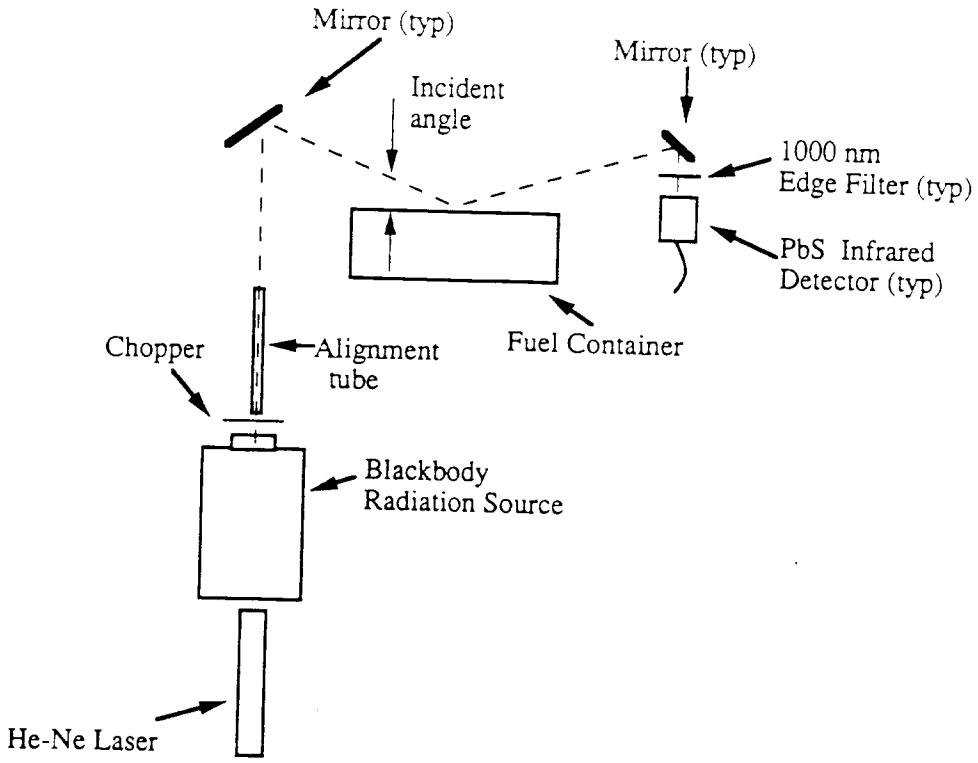

FIGURE 5 A schematic drawing of the experimental set-up for measuring the radiative flux reflected from the pool surface.

the simple burner was utilized. The gauge was positioned at the plane defined by the lip of the burner. Data was sampled at a rate of 30 Hz for 90 seconds per location. During the experiment, increases on the order of 3 K were observed in the temperature of the heat flux gauge cooling water. The effect of this heat up on detector output was tested by increasing the temperature of the cooling water with the gauge facing a black body source (1273 K). It was determined that heating the cooling water as much as 5 K had a negligible effect on the detector output. Heat flux measurements along the fuel surface were repeated at least twice for each fuel. Calibration was achieved using a tungsten lamp light source and a standard gauge. Repetition of the tests indicated that the uncertainty in the signal output was approximately 10%.

A video record of the fires (30 frames/second) was used to determine flame heights and pulsation frequencies.

2.4 *Conductive Heat Transfer*

Heat loss to the cooling water at the bottom of the pool burner was monitored by measuring the volumetric flow of water and the temperatures at the water inlet and outlet at the burner bottom. Conductive heat transfer from the flame through the walls of the rings was estimated by measuring the temperature of thermocouples which had

been spot-welded 0.1 and 0.4 cm below the top of a thin steel bar and placed inside of the simple burner pool, with the top of the bar at the plane defined by the burner rim. The temperature on the bar was monitored as the bar was moved through the pool.

3. EXPERIMENTAL RESULTS

3.1 Flame Character

Global combustion characteristics for 0.30 m pool fires burning toluene, heptane, MMA and methyl alcohol are listed in Table I, including the mass burning rate ($\dot{m}$, the heat feedback fraction (χ_s), the idealized combustion heat release rate ($\dot{Q}_{chem}$), the rate of radiative heat loss from the flame to the surroundings ($\dot{Q}_{emit}$), the radiative heat loss fraction (χ_R) which was measured previously (Hamins et al., 1991), the measured average flame height (H_{exp}) and the average flame heights (H_z and H_H) determined from the correlations given by Zukoski (1984) and Heskestad (1983). Figures 6 and 7 are photographs of 0.30 m diameter pool fires burning methyl alcohol and heptane, respectively. Differences in the radiative emission characteristics of the fires burning these two fuels can be attributed to the presence of a significant concentration of soot particles in the heptane fire. Gaseous species emit radiation in the heptane fire, but the visible radiation intensity emitted by soot far exceeds that of gaseous emission. Whereas the idealized heat release rate from the methyl alcohol fire is a factor of five less than the heptane fire, the radiation emitted to the surroundings ($\dot{Q}_{emit}$) from the methyl alcohol fire is about an order of magnitude less than from the heptane fire.

The visible average height of the pool fires was also dependent on fuel type. Table I shows that the time-averaged flame heights for heptane were the largest, followed by toluene, MMA and methyl alcohol. Average visible flame heights were approximately the same in the 0.30 m simple and 0.30 m ring burner and in general, the rings appeared to have little impact on the flame shape, overall burning rate, or shape of the fires. Comparison of experimental measurements with the correlations given by Heskestad (1983) and Zukoski (1984) showed that they were fairly accurate, except for the case of toluene where the mean flame height was over-predicted by 25% and 32% respectively. These correlations were apparently developed, however, without consideration for variations in radiative heat loss fraction or combustion efficiency, which vary with fuel type, fire scale and oxygen mass fraction in the oxidizer. When the combustion efficiency of toluene, taken to be 0.70 (Tewarson, 1988), was considered, the correlations were more accurate, slightly over-predicting the average toluene flame height by 4% and 15%.

The shape of the methyl alcohol fire was unusual when compared to those of the other fuels in this study. The methyl alcohol flame shape changed dramatically with time through a pulsation cycle, with the necking-in or lateral extent of the flame changing from approximately 0.8 to 0.4 times the diameter. A series of thin blue flame sheets swept radially inward across the fuel surface in what appeared to be waves. The heptane, MMA and toluene fires did not exhibit large necking-in regions. These fires were turbulent and had a time-averaged flame shape that could be characterized as approximately cylindrical.

Examination of the video record for the methyl alcohol fires shows that at steady burning conditions the characteristic pulsation frequency for the 0.30 m diameter pool was approximately 2.8 ± 0.3 Hz. This was consistent with previous studies (Hamins et al., 1992) and was in accord with a spectral analysis of thermocouple data (0.005 cm diameter Chromel-Alumel) taken in the fire at a location one radius above the pool surface and 7.5 cm laterally from the pool center. In addition, standing waves were observed on the surface of the methyl alcohol pool and were measured to have a characteristic frequency of 2.0 ± 0.2 Hz. The similarity in the frequency of gas and liquid phase phenomena

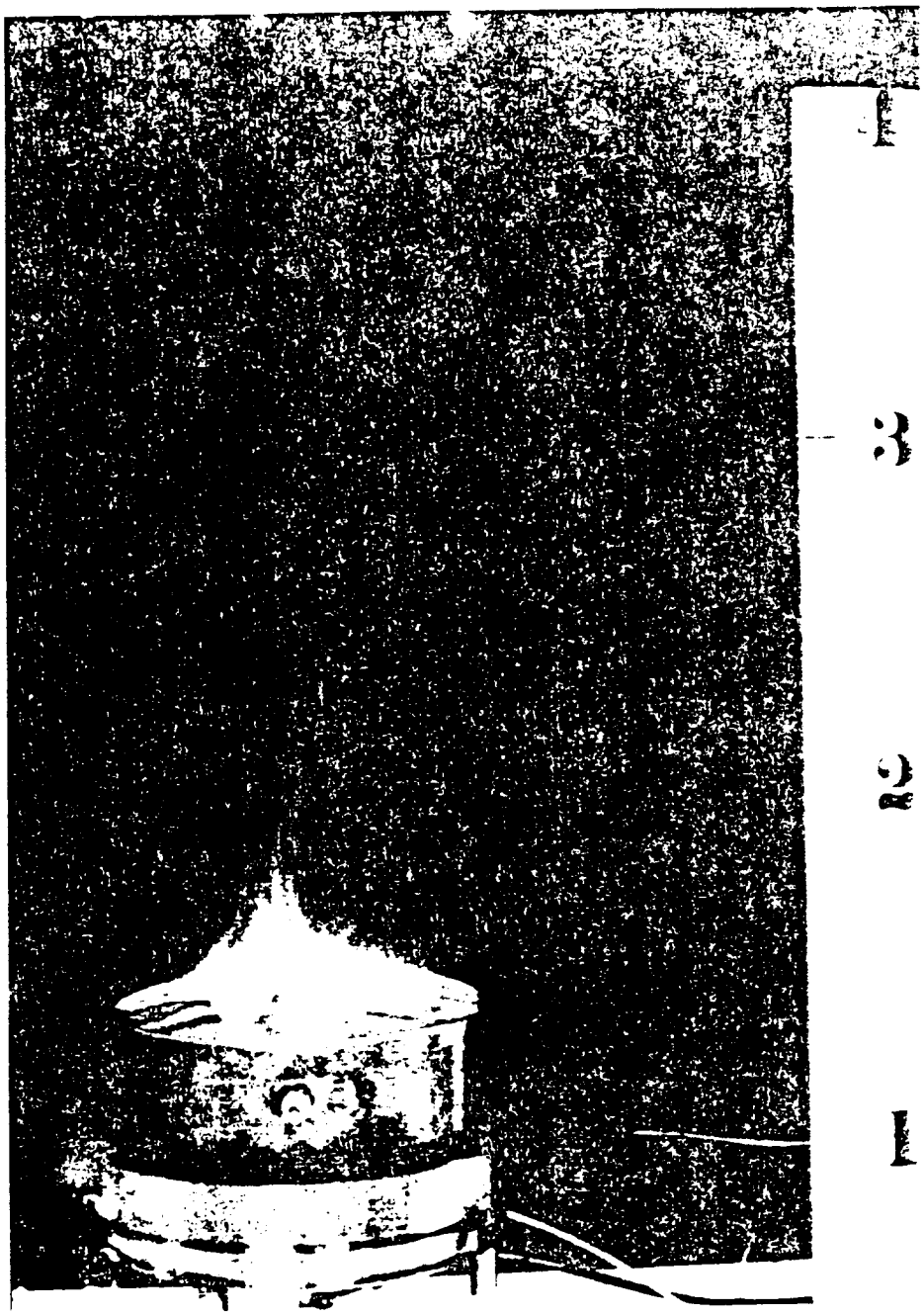

FIGURE 6. Photograph of a 1.0 diameter pool fire burning methyl alcohol. The side scale is marked in increments of 1 foot (0.3 m). See COLOR PLATE I.

FIGURE 7 Photograph of a 0.30 diameter pool fire burning heptane. The side scale is marked in increments of 1 foot (0.3 m). See COLOR PLATE II.

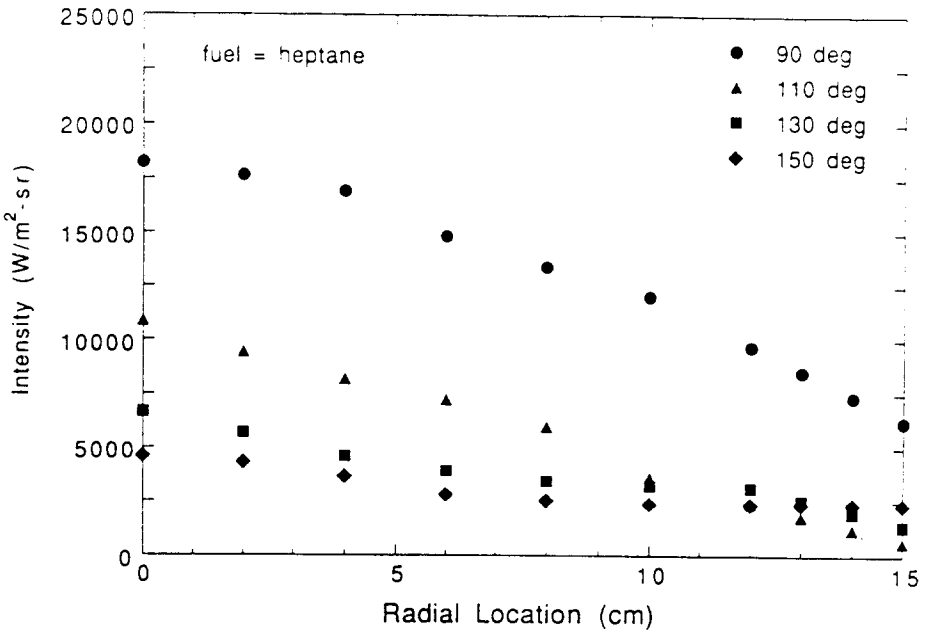

FIGURE 8 The time-averaged radiative intensity as a function of radial location on the surface of the 0.30 m pool burning heptane for directions defined by ϕ = 90°, Θ = 90°, 110°, 130°, and 150°. The center of the pool is indicated by the 0 cm position.

suggests that the momentum associated with the pulsations in the gas phase exert a perturbation on the methyl alcohol pool (Hamins et al., 1992). Some damping of the perturbation may be caused by liquid viscosity. These observations are consistent with measurements reported by Cetegen and Ahmed (1990) who measured regular pressure fluctuations at the surface of pool fires correlated with the natural puffing frequency. Surface standing waves have not been reported previously nor were they observed in fires burning any of the other fuels. This was associated with the coherent nature of the pulsing methyl alcohol fire.

Observation of the video film record reveals a number of other prominent fire characteristics. The heptane fire was much wider than the MMA fire. The time-averaged lateral extent of the (simple burner) heptane fire at one diameter above the pool was 0.32 m, while the MMA fire was 0.21 m. This observation was consistent with the higher oxygen demand of the heptane fire compared to the partially-oxygenated MMA. Whereas both fuels had the same molecular weight and approximately the same burning rate (see Table I), the air necessary for stoichiometric burning of heptane is almost a factor of 2 larger than MMA.

The methyl alcohol fire shown in Fig. 6 was a blue, non-sooty flame, with radiation originating from emission by high temperature gaseous species. Fires of toluene, MMA and heptane yielded luminous yellow flames. Large differences in the power emitted to the surroundings ($\dot{Q}_{emit}$) by these pool flames have been reported (Hamins et al., 1991) as shown in Table I where $\dot{Q}_{emit}$ (W) was defined as:

$$\dot{Q}_{emit} = \dot{Q}_{chem} \cdot \chi_R \tag{6}$$

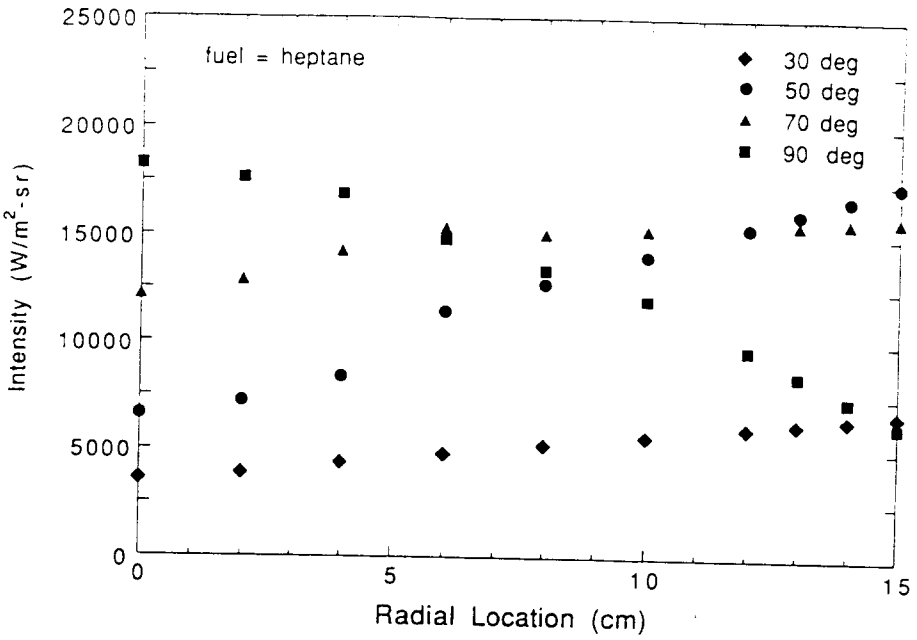

FIGURE 9 The time-averaged radiative intensity as a function of radial location on the surface of the 0.30 m pool burning heptane for directions defined by $\phi = 90°$ and $\Theta = 30°$, 50°, 70°, and 90°. The center of the pool is indicated by the 0 cm position.

$\dot{Q}_{emit}$ was largest for the toluene fire and almost an order of magnitude smaller for the methyl alcohol fire. Table I shows that the average mass burning rates ($\dot{m}$) in the pool increased with increasing radiated power ($\dot{Q}_{emit}$). This correlation indicates the importance of radiation in the heat feedback process. Yet, other factors such as radiation blockage by gas species and soot particles could play an important role. Thus, direct detailed measurements of the radiative heat feedback were necessary to determine the relative importance of radiation and convection in these fires.

3.2 Radiative Heat Flux Measurements

Figure 8 shows the time-averaged radiative intensity as a function of radial locations on the surface of the 0.30 m pool burning heptane for directions defined by $\phi = 0°$ and $\Theta = 90°$, 110°, 130°, and 150°. Figure 9 shows its value for directions defined by $\phi = 0°$ and $\Theta = 30°, 50°, 70°$ and 90°. The radial positions designated as 15 and 0 cm refer respectively to the edge and center of the pool. In Fig. 8, the intensity was largest for the $\Theta = 90°$ direction and the intensity for all directions directed away from the central axis decreased for locations towards the edge of the pool. In Fig. 9, the intensity in the $\Theta = 30°$ and 50° directions increased for locations towards the pool edge. The results in Figs. 8 and 9 were consistent with a roughly cylindrical flame shape. Similar measurements were also made in the $\phi = 90°$ direction (as described in Section 2.2). Analogous measurements were conducted in fires burning toluene (Klassen et al., 1992) and methyl alcohol.

The radiation intensities shown in Figs. 8 and 9 were used to determine the incident radiative heat flux, $\dot{Q}''_{rad}(r)$, as a function of location on the pool surface as shown in

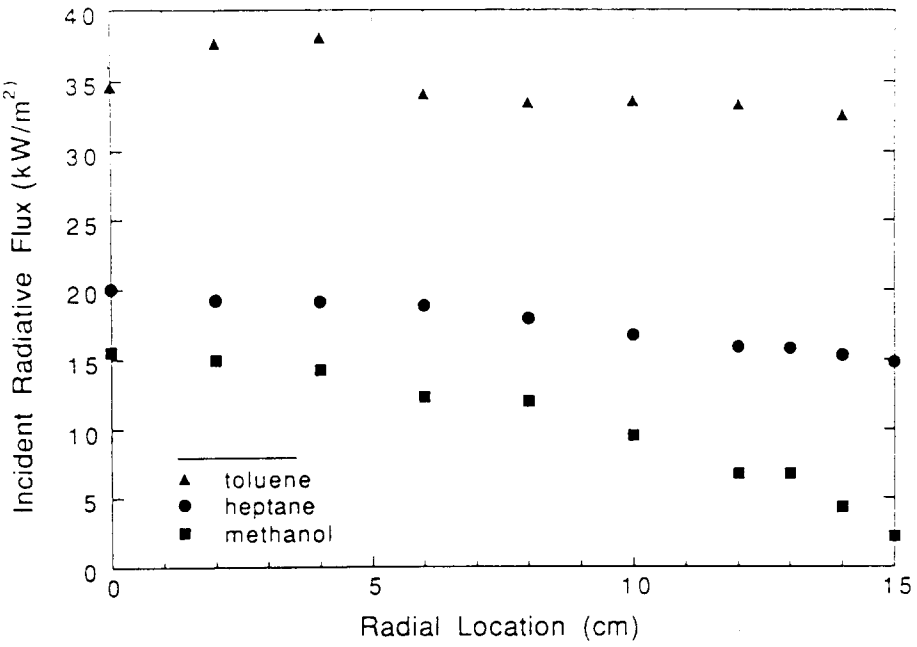

FIGURE 10 Incident radiative heat flux as a function of location on the surface of 0.30 m pool fires burning toluene, heptane and methyl alcohol.

Fig. 10. The double prime (″) represents quantities per unit pool surface area. $\dot{Q}''_{rad}(r)$ was determined using symmetry, the trapezoidal rule, and by integrating the intensity, $I(r,\Theta,\phi)$, about the hemisphere above each radial location (r) on the pool surface:

$$\dot{Q}''_{rad}(r) = \int\int I(r,\Theta,\phi)\cos(\Theta)\sin(\Theta)d\Theta d\phi \qquad (7)$$

where the direction angles Θ and ϕ are defined in Fig. 4. Figure 10 shows that the radiative heat flux was largest for the toluene fire followed by heptane and methyl alcohol. The radiative flux was essentially flat across the pool surface for the toluene fire, decreased slightly for the heptane fire and decreased sharply toward the edge for the methyl alcohol fire.

3.3 Measurement of Reflected Radiation

Figure 11 shows measurements of the ratio of the reflected to incident radiative flux as a function of incident angle for the three liquid fuels and water. Also shown are curves calculated from a solution of the Fresnel equations in conjunction with Snell's Law for refractive indices (N) equal to 1.4 and 1.5. The measurements for all fuels were nearly represented by the N=1.5 curve. The reflected radiation was used to deduce the absorbed radiative flux into the pool and proved to be a non-negligible contribution to the overall heat balance.

3.4 Absorbed Radiation

The radiative flux absorbed by the pool was defined as the difference between the incident

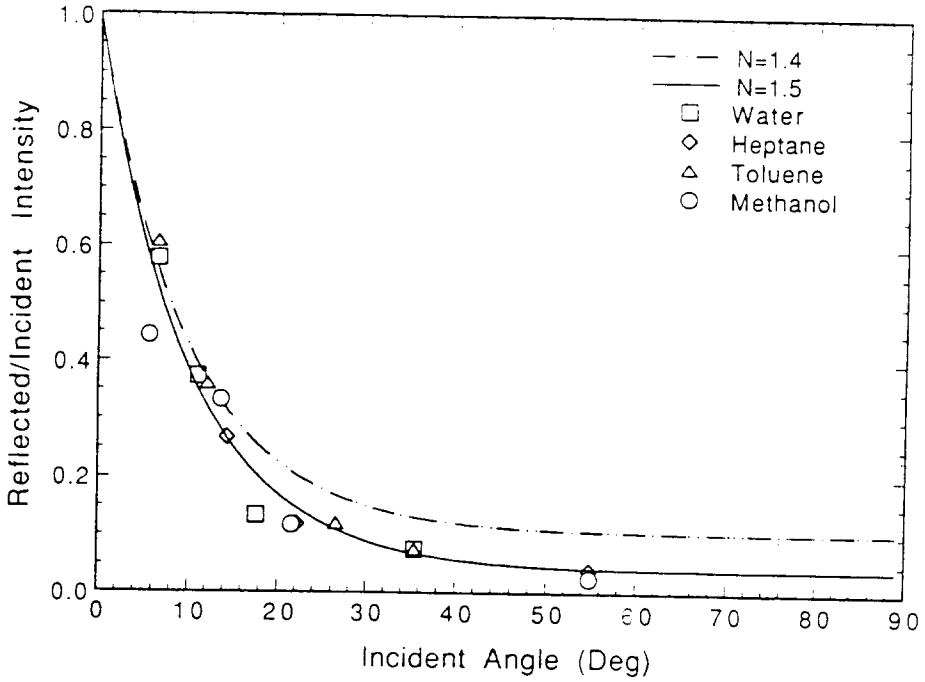

FIGURE 11 Measured values of the ratio of the reflected to incident radiative flux as a function of incident angle for water, methyl alcohol, heptane and toluene. Calculated curves for indices of refraction (N) equal to 1.4 and 1.5 are also shown.

and reflected radiative fluxes:

$$(\dot{Q}''_{rad} - \dot{Q}''_{reflect}) = \int\int I(r,\phi,\Theta)[1 - R(\Theta)]\cos(\Theta)\sin(\Theta)d\Theta d\phi \qquad (8)$$

where R(Θ) was the normalized reflected radiation shown in Fig. 11, assuming that all fuels behaved like a material with a refractive index of N=1.5. The [1-R(Θ)] term diminished by 5 to 8% the amount of incident radiative flux absorbed by the pool, with slightly more reflection occurring at the edge than at the pool center. Some variation occurred with different fuels due to differences in flame shape.

3.5 Local Mass Burning Rates

Figure 12 shows the mass burning rate as a function of time for the five-ring pool fire burning heptane. After 500 seconds, each of the curves appears linear, indicating that a steady state mass burning rate was attained in each of the rings. This is in contrast to pool fires burning solid fuels where steady state burning can take much longer to attain (Modak and Croce, 1977) and to pool fires where the fuel level is not maintained constant and the burning rate shows variation throughout the experiment (Shinotake et al., 1985).

Figure 13 shows the average mass flux or burning rate as a function of ring number for pool fires burning methyl alcohol, MMA, toluene, and heptane in a four-ring and

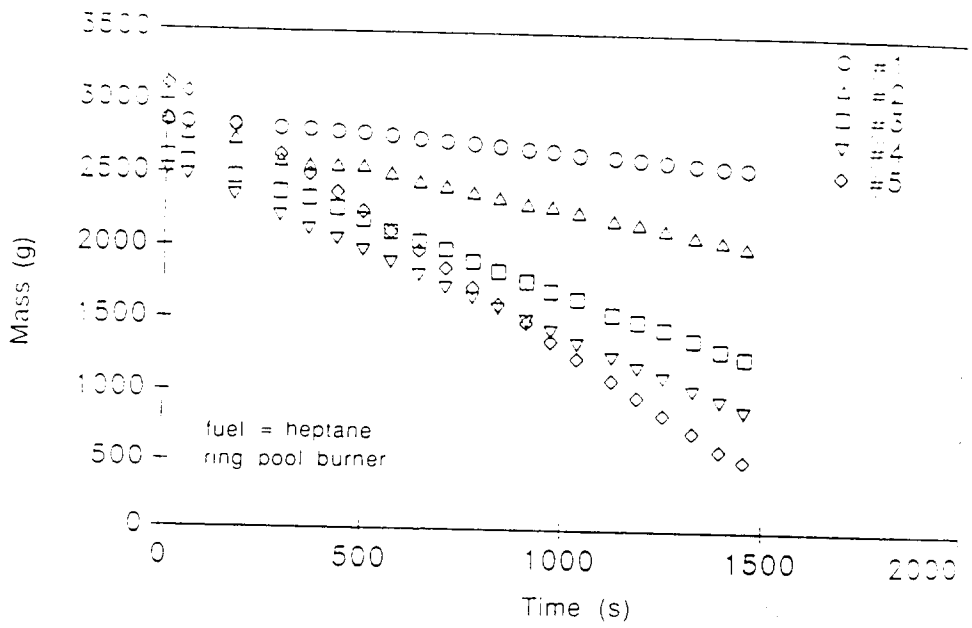

FIGURE 12 Mass burning rates as a function of time for each ring in a five-ring 0.38 m diameter pool fire burning heptane.

heptane in a five-ring configuration. In this figure, all fires were maintained with a 0.5 cm lip height. For all fuels tested, the highest mass burning rate was for the inner ring. Methyl alcohol has the smallest mass burning rate while the largest mass burning rate on average was that of toluene followed by MMA and heptane. The heptane fire with a fifth fuel ring (outer diameter = 0.38 m) has almost a 20% faster burning rate than the four-ring (outer diameter = 0.30 m) heptane fire. Local heat feedback measurements with a Gardon type gauge are shown in Figs. 14-16 for pool fires burning heptane, toluene, and MMA respectively in the simple pool burner. Superimposed on these results are the net heat feedback calculated from the mass burning rate measurements shown in Fig. 13. The lateral extent of the rings in Figs. 14-16 are denoted by the horizontal bars. Heat feedback for the rings can be thought of as an average heat flux centered about the data point.

Good agreement was found between the heat flux calculated from the ring burning rate data and the heat flux gauge data as a function of location on the surface of the heptane pool as shown in Fig. 14. The measured heat flux decreases from the center outward and then rises near the edge of the pool. Figure 15 shows results for the toluene fire. Typical uncertainty in the local heat flux measurements is shown in the figure. The inner ring burning rate measurement was inconsistent with the Gardon gauge result. This was attributed to difficulties in maintaining the liquid level in the inner-most ring in the toluene fire - where visible observation of the liquid level was obscured by intense flame luminosity. For the other rings in the toluene fire, the heat fluxes calculated from the measured burning rates were consistent with heat fluxes measured by the Gardon gauge. A slight increase in heat flux near the pool edge was exhibited by these data, which is in accord with the ring burning rate results. Figure 16 shows the heat flux to

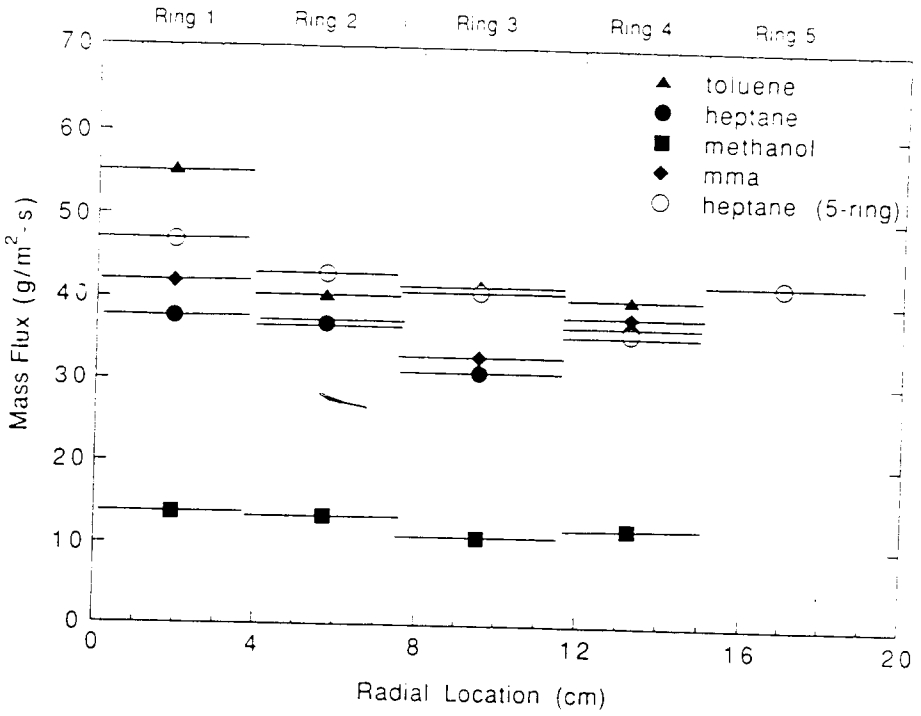

FIGURE 13 Time-averaged mass burning rate as a function of ring location for pool fires burning methyl alcohol, MMA, toluene, and heptane in a four-ring and heptane in a five-ring pool.

the surface of the MMA pool fire, which decreased slightly from the center towards the pool edge. The heat flux measurements were in fair agreement with the ring burning rate results except near the pool edge, where the mass burning rates in the ring burner yielded higher results.

3.6 *Comparison of Burning Rate Measurements with Previous Work*

In a series of square pool fires burning polymethylmethacrylate (PMMA), Modak and Croce (1977) measured a monotonic decrease in burning rate from pool center to pool edge. For a PMMA square (0.31 m × 0.31 m), the local burning rate at the pool edge was approximately half the burning rate at the pool center. In our MMA fire, the rate of burning at the pool edge was about 90% of the rate at pool center. The composition of chemical intermediates in a small PMMA flame has been shown to be highly similar to the composition of a flame burning its liquid monomer, MMA (Seshadri, 1976). Yet, differences exist in the surface temperature of these two fuels, their burning rates, flame shapes and χ_s. These factors could lead to large differences in the relative importance of local radiative and convective heat transfer. Thus, differences in the burning rate profiles along the pool surface between the ring pool mass burning rate measurements shown in Fig. 13 and the results of Modak and Croce (1977) are not entirely surprising.

Figure 17 compares the mass flux results of Akita and Yumoto (1965) for their 0.29 m diameter pool fire burning methyl alcohol to the mass flux measurements in the 0.30 m diameter pool plotted as a function of location for each ring. The lateral extent of each

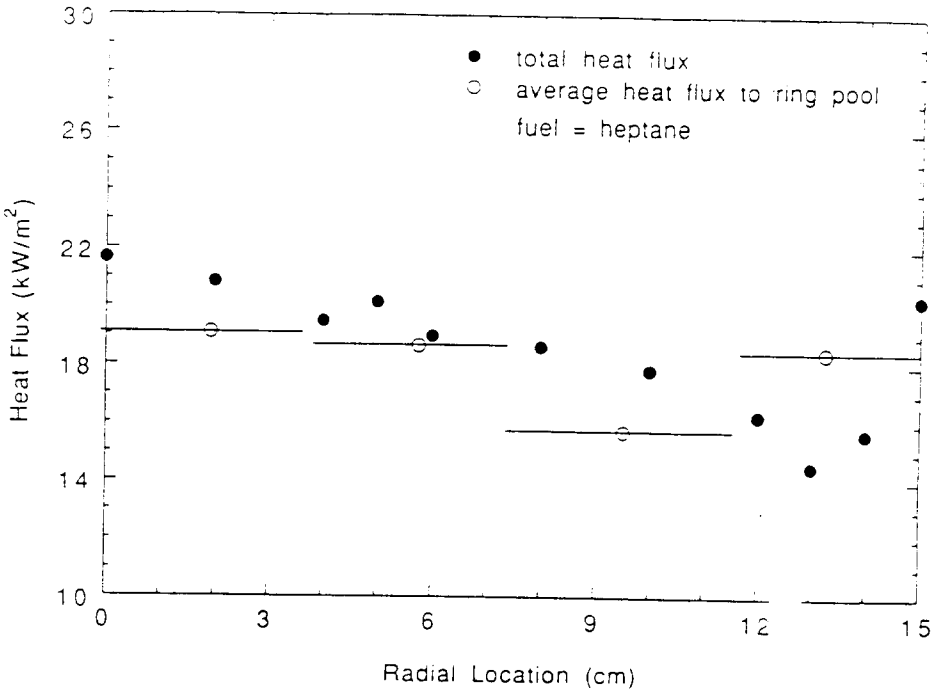

FIGURE 14 Local heat feedback measurement as a function of radial location for a 0.30 m pool fire burning heptane. Also shown are the net heat feedback calculated from mass burning rates in annular rings (see Fig. 13). The lateral extent of the rings are denoted by the horizontal bars.

ring is indicated by the horizontal bar associated with each data point. Whereas Akita and Yumoto (1965) utilized a three-ring pool, each ring having equal area, the present experiments were conducted in a four-ring pool with equal spacing between rings. The area of the inner ring used by Akita and Yumoto (1965) was approximately equal to the area of the innermost two rings used here. The outer two rings had approximately the same area. A comparison of the present results with those of Akita and Yumoto (1965) show different methyl alcohol burning rates in both magnitude and profile. The present results at the pool center were approximately fifty percent larger. Whereas the present mass flux measurements decreased from the pool center towards the edge, Akita and Yumoto (1965) reported increased mass flux towards the pool edge. Lip height conditions for the experiments of Akita and Yumoto (1965) are not available. In order to insure that differences in the burning rate data were not attributable to differences in lip height, measurements were conducted for two different lip heights (with the fuel level at 0.1 and 0.5 cm below the burner rim). The results indicate that the differences in burning rate cannot be accounted for by the effect of lip height. Figure 17 shows that the profile of burning rate decreased monotonically for methyl alcohol burning with a 0.5 cm lip, whereas the profile with a 0.1 cm lip decreased and then increased near the pool rim. The difference in the shape of these profiles may indicate the importance of convection near the burner rim.

Burning rate measurements were also conducted with a fifth ring filled with water (initially at ambient temperature) - similar to the conditions used by Akita and Yumoto. The burning rates for each of the rings showed negligible difference from measurements

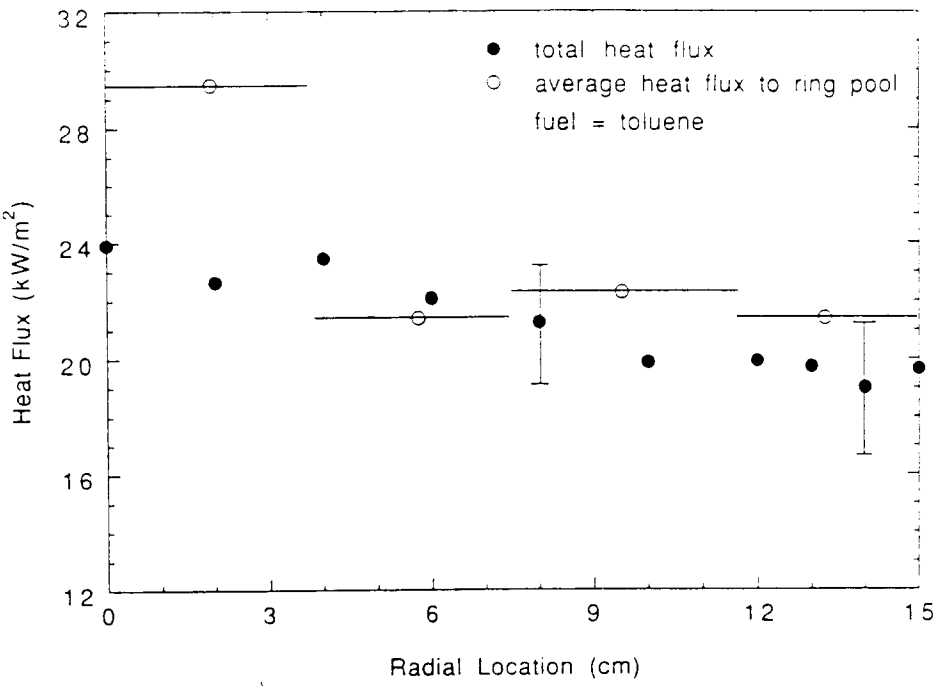

FIGURE 15 Local heat feedback measurement as a function of radial location for a 0.30 m pool fire burning toluene. Also shown are the net heat feedback calculated from mass burning rates in annular rings (see Fig. 13). The lateral extent of the rings are denoted by the horizontal bars.

made without the extra water-filled ring. Thus, the measurements reported by Akita and Yumoto (1965) could not be repeated. Furthermore, Akita and Yumoto's conclusion that radiation played no role in the non-luminous methyl alcohol pool fires appear unsupported in light of the radiation measurements discussed below.

3.7 *Estimate of the Normalized Radiative Heat Flux*

Evaluation of the portion of the local heat feedback that was due to radiative heat transfer required an estimate of the steady local net heat flux ($\dot{Q}''_{net,i}$) incident on the fuel surface. $\dot{Q}''_{net,i}$ was estimated by applying Eq. 5 to each ring in the ring pool burner:

$$\dot{Q}''_{net,i} = \dot{Q}''_{fuel,i} + \dot{Q}''_{rerad} + \dot{Q}''_{loss} + \dot{Q}''_{corr} \tag{9}$$

$$with\ \dot{Q}''_{fuel,i} = \dot{m}''_i \cdot (H_v + C_p \cdot [T_s - T_o]) \tag{10}$$

where $\dot{Q}''_{net,i}$ was the average heat flux incident on the i^{th} ring. H_v, C_p, T_s and T_o were defined earlier. In order to estimate $\dot{Q}''_{net,i}$ the terms on the right hand side of Eq. 9 had to be evaluated. $\dot{m}''_i$ was the average measured mass burning rate ($\dot{m}$) per unit area in the i^{th} ring.

Estimate of the normalized radiative portion of the local heat feedback was based on a correspondence between the radiation measurements made in the 0.30 diameter

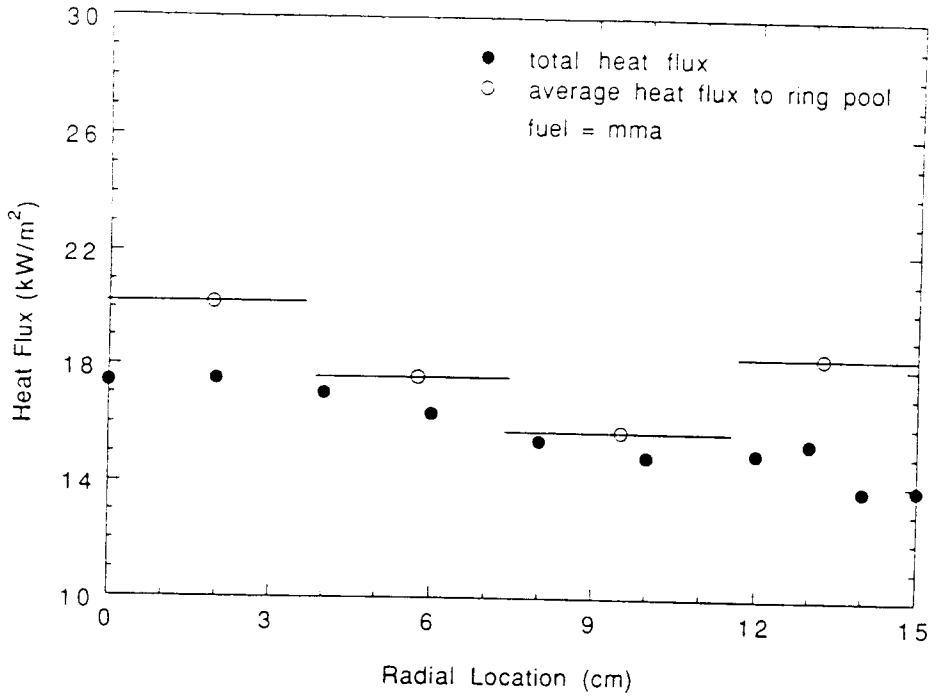

FIGURE 16 Local heat feedback measurement as a function of radial location for a 0.30 m pool fire burning MMA. Also shown are the net heat feedback calculated from mass burning rates in annular rings (see Fig. 13). The lateral extent of the rings are denoted by the horizontal bars.

simple burner and the net heat flux measurement determined by the mass burning rate measurements in the 0.30 m diameter ring burner. Fuel lip heights were minimized (0.5 cm) for the tests in order to diminish the effect of the metal rings. The conductive heat transfer from the flame through the walls of the rings as described in Section 2.4 was estimated to be small. Finally, the average flame heights, average total burning rates ($m_{\text{simple burner}} \approx \Sigma m_{\text{ring burner},i}$), and the general appearance of the fires were highly similar. Possible differences in liquid phase fluid motion in the burners, due to the absence or presence of the annular rings, had little apparent effect on the heat transfer processes governing the fuel burning rate. In general, the rings appeared to have little impact on the character of the fires. The data presented in Figs. 14-16 further support the correspondence between the burners by showing that the local net heat feedback had approximately the same absolute value and slope as a function of radial location in both pools.

The terms $\dot{Q}''_{\text{rerad}}$, $\dot{Q}''_{\text{loss}}$, and $\dot{Q}''_{\text{corr}}$ in Eq. 9 were appraised as follows; $\dot{Q}''_{\text{loss}}$ was measured and then divided by the pool surface area, effectively treating the loss as uniform over the pool surface.

The average heat loss to the surroundings by surface re-radiation per unit pool surface area ($\dot{Q}''_{\text{rerad}}$), was estimated as:

$$\dot{Q}''_{rerad} = \varepsilon\sigma T^4 \tag{11}$$

where the emissivity (ε) of the pool surface was taken as 1.0, the pool surface temperature was assumed to be equal to the fuel boiling temperature, and the Stefan-Boltzman

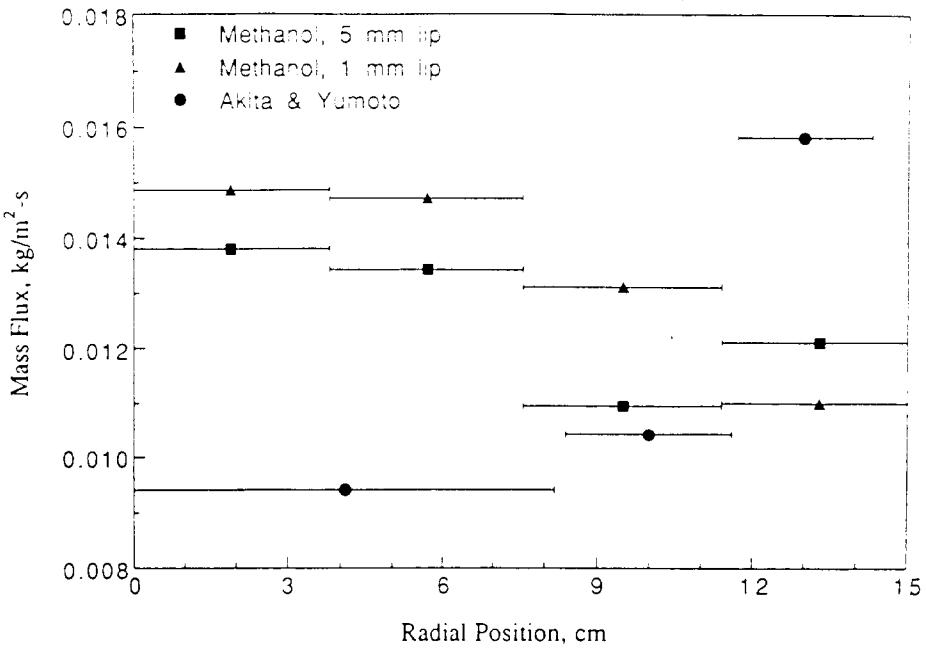

FIGURE 17 Mass burning rates as a function of radial location for methyl alcohol burning in a 0.30 m ring pool with 0.1 and 0.5 cm lip heights. Also shown are results reported by Akita and Yumoto (1965).

constant, $\sigma = 5.67 \cdot 10^{-8} W/m^2 - K^4$. The re-radiation term for the methyl-alcohol fire was estimated to be approximately one-half that of the heptane or toluene fires, due to its low boiling point, 338 K, as compared to 372 K for heptane and 384 K for toluene (Gallant, 1968).

The temperature inside of the liquid pool gradually increased with time. Figure 18 shows the change in temperature at three locations inside the pool for a methyl alcohol fire established in the simple burner. The time rate of change in temperature (dT(z)/dt) at a distance (z) from the pool surface approached a constant value during the warmup period, typically within 100 s after ignition. The heat flux that went to raise the temperature of the fuel inside of the liquid pool ($\dot{Q}''_{corr}$) was estimated by integrating the rate of temperature change through the pool depth (0.15 m), assuming a one-dimensional temperature profile and using data such as that shown in Fig. 18:

$$\dot{Q}''_{corr} = \int \rho(z) \cdot C_p(z) \cdot (dT(z)/dt) dz \tag{12}$$

where $\rho(z)$ and $C_p(z)$ are the density and heat capacity of the liquid fuel and z is the distance below the fuel surface (Gallant, 1968).

Table IV shows that the relative importance of $\dot{Q}''_{rerad}$, $\dot{Q}''_{loss}$, and $\dot{Q}''_{corr}$ varied from flame to flame, taking on values from 0.5 to 12% of the $\dot{Q}''_{fuel,i}$.

Corresponding to Eq. 4, the local heat flux was defined as:

$$\dot{Q}''_{net}(r) = \dot{Q}''_{cond}(r) + \dot{Q}''_{conv}(r) + \dot{Q}''_{rad}(r) - \dot{Q}''_{reflect}(r) \tag{13}$$

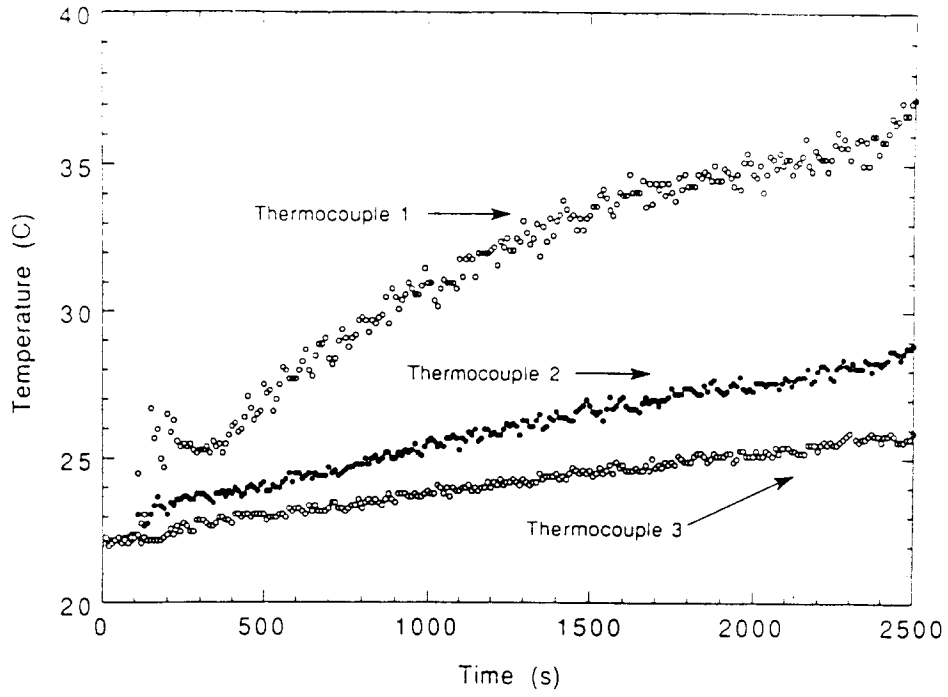

FIGURE 18 Temperature profiles inside a burning pool of liquid methyl alcohol. Thermocouples (#1, 2 and 3) placed 1.5, 4, and 8 cm (respectively) below the fuel surface.

The conductive heat transfer through the burner walls, per unit pool surface area ($\dot{Q}''_{cond}$), was estimated to be ≈ 0.3 kW/m^2 (based on the measurements described in Section 2.4) which was a small fraction of the net heat feedback for all fuels.

The local net heat flux $\dot{Q}''_{net}(r)$ was estimated from smoothing the data determined using Eq. 9. Figure 19 shows the measured local absorbed radiative heat flux (Eq. 8) normalized by the local net heat flux $\dot{Q}''_{net}(r)$. For the toluene fire, the values of $\dot{Q}''_{net}(r)$ were multiplied by a factor of 1.33 to account for the enhanced burning rate, which was 33% higher for the radiative heat flux measurements than for the ring pool burning rate measurements, due to the hot water used to cool the radiative heat flux gauge. The difference between the normalized absorbed radiative flux and a value of unity was attributed to convective heat transfer and a very small amount of conduction near the burner rim. The heat feedback to both luminous and non-luminous fires was radiation dominated near the pool center. The intensity profile of normalized absorbed radiative flux was flat in the toluene fire, was highest near the pool center and decreased somewhat towards the fuel edge in the heptane fire, and showed a steep decrease from pool center towards the edge in the methyl alcohol fire. Integration of the curves yielded values of approximately 96%, 80% and 55% for the radiative portion of the heat feedback to the pool surface ($\dot{Q}''_{rad}/\dot{Q}''_{net}$) for the toluene, heptane, and methyl alcohol fires respectively.

Water condensation in the fuel ($\dot{Q}''_{water}$) is expected to be of negligible importance in the heat balance for the heptane and toluene fires, but may be non-negligible in the methyl alcohol fire with its relatively low boiling temperature. Extrapolating the data from Corlett and Fu (1966), an estimate of the effect of water condensation on

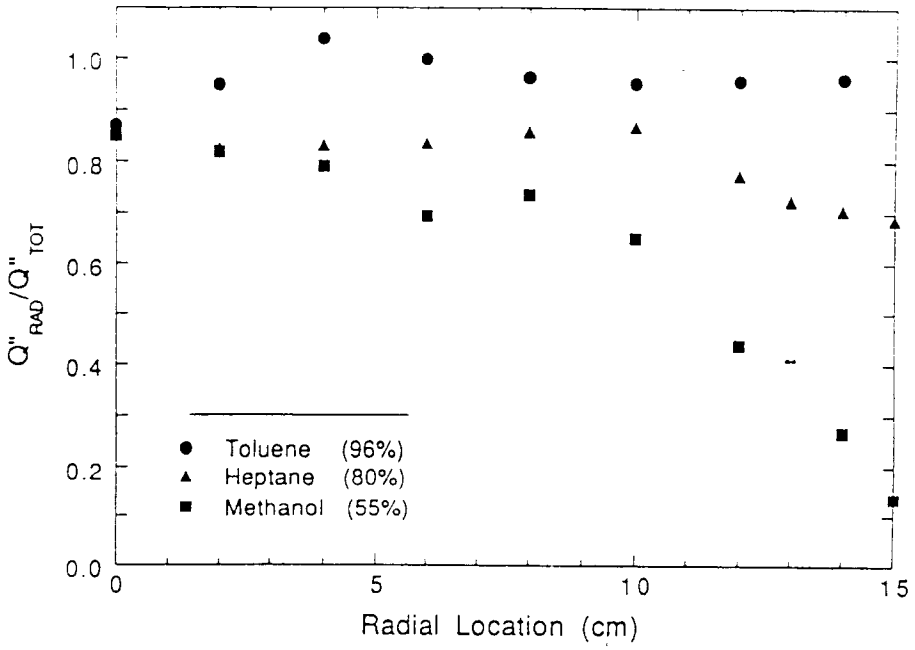

FIGURE 19 The absorbed radiative heat flux normalized by the local net heat flux as a function of location on the surface of 0.30 m pool fires burning toluene, heptane and methyl alcohol. Numbers in parenthesis indicate the percentage of heat feedback which was due to radiation.

TABLE IV

The ratio of minor heat loss terms: $\dot{Q}''_{rerad}$, $\dot{Q}''_{loss}$, and $\dot{Q}''_{corr}$ to the dominant loss term $\dot{Q}''_{fuel,i}$.

Fuels	$\dot{Q}''_{rerad}/\dot{Q}''_{fuel,i}$	$\dot{Q}''_{loss}/\dot{Q}''_{fuel,i}$	$\dot{Q}''_{corr}/\dot{Q}''_{fuel,i}$
methyl alcohol	0.02	0.01	0.005
heptane	0.04	0.03	0.04
toluene	0.04	0.06	0.12

the heat balance in the methyl alcohol fire yielded a small decrease in the radiative portion of the heat feedback ($\dot{Q}''_{rad}/\dot{Q}''_{net}$) to 53% from 55%. Including or neglecting water condensation, radiative heat transfer played an important role in the heat feedback to the methyl alcohol pool fire, in contrast with the conclusions suggested by Akita and Yumoto (1965).

4. SUMMARY AND CONCLUSIONS

A series of measurements were conducted in 0.30 m pool fires to determine the portion of the energy feedback due to radiation as well as the spatial variation of the radiated energy along the pool surface. The key conclusions are:

1. Radiation plays an important if not dominant role in the heat feedback to 0.30 m pool fires for both luminous and non-luminous fuels.